

---

## Finite-Volume Methods

Finite-volume methods (FVM) – sometimes also called box methods – are mainly employed for the numerical solution of problems in fluid mechanics, where they were introduced in the 1970s by McDonald, MacCormack, and Paullay. However, the application of the FVM is not limited to flow problems. An important property of finite-volume methods is that the balance principles, which are the basis for the mathematical modelling of continuum mechanical problems, per definition, also are fulfilled for the discrete equations (conservativity). In this chapter we will discuss the most important basics of finite-volume discretizations applied to continuum mechanical problems. For clarity in the presentation of the essential principles we will restrict ourselves mainly to the two-dimensional case.

### 4.1 General Methodology

In general, the FVM involves the following steps:

- (1) Decomposition of the problem domain into control volumes.
- (2) Formulation of integral balance equations for each control volume.
- (3) Approximation of integrals by numerical integration.
- (4) Approximation of function values and derivatives by interpolation with nodal values.
- (5) Assembling and solution of discrete algebraic system.

In the following we will outline in detail the individual steps (the solution of algebraic systems will be the topic of Chap. 7). We will do this by example for the general stationary transport equation (see Sect. 2.3.2)

$$\frac{\partial}{\partial x_i} \left( \rho v_i \phi - \alpha \frac{\partial \phi}{\partial x_i} \right) = f \quad (4.1)$$

for some problem domain  $\Omega$ . We remark that a generalization of the FVM to other types of equations as given in Chap. 2 is straightforward (in Chap. 10 this will be done for the Navier-Stokes equations).

The starting point for a finite-volume discretization is a decomposition of the problem domain  $\Omega$  into a finite number of subdomains  $V_i$  ( $i = 1, \dots, N$ ), called *control volumes* (CVs), and related nodes where the unknown variables are to be computed. The union of all CVs should cover the whole problem domain. In general, the CVs also may overlap, but since this results in unnecessary complications we consider here the non-overlapping case only. Since finally each CV gives one equation for computing the nodal values, their final number (i.e., after the incorporation of boundary conditions) should be equal to the number of CVs. Usually, the CVs and the nodes are defined on the basis of a numerical grid, which, for instance, is generated with one of the techniques described in Chap. 3. In order to keep the usual terminology of the FVM, we always talk of volumes (and their surfaces), although strictly speaking this is only correct for the three-dimensional case.

For one-dimensional problems the CVs are subintervals of the problem interval and the nodes can be the midpoints or the edges of the subintervals (see Fig. 4.1).

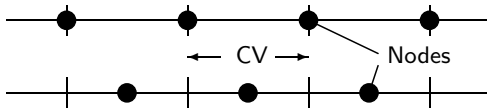


**Fig. 4.1.** Definitions of CVs and edge (top) and cell-oriented (bottom) arrangement of nodes for one-dimensional grids

In the two-dimensional case, in principle, the CVs can be arbitrary polygons. For quadrilateral grids the CVs usually are chosen identically with the grid cells. The nodes can be defined as the vertices or the centers of the CVs (see Fig. 4.2), often called edge or cell-centered approaches, respectively. For triangular grids, in principle, one could do it similarly, i.e., the triangles define the CVs and the nodes can be the vertices or the centers of the triangles. However, in this case other CV definitions are usually employed. One approach is closely related to the Delaunay triangulation discussed in Sect. 3.4.2. Here, the nodes are chosen as the vertices of the triangles and the CVs are defined as the polygons formed by the perpendicular bisectors of the sides of the surrounding triangles (see Fig. 4.3). These polygons are known as *Voronoi polygons* and in the case of convex problems domains and non-obtuse triangles there is a one-to-one correspondance to a Delaunay triangulation with its “nice” properties. However, this approach may fail for arbitrary triangulations. Another more general approach is to define a polygonal CV by joining the centroids and the midpoints of the edges of the triangles surrounding a node leading to the so-called *Donald polygons* (see Fig. 4.4).

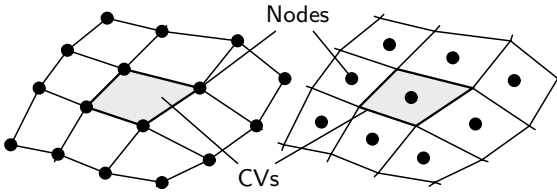


**Fig. 4.2.** Edge-oriented (left) and cell-oriented (right) arrangements of nodes for quadrilateral grids

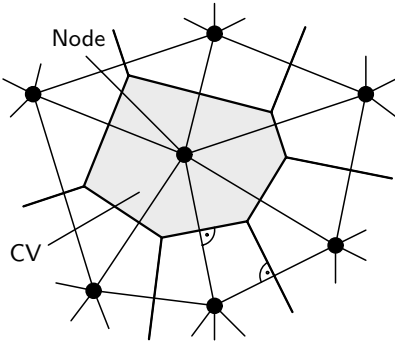


**Fig. 4.3.** Definition of CVs and nodes for triangular grids with Voronoi polygons

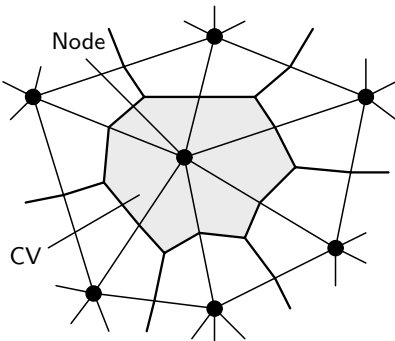


**Fig. 4.4.** Definition of CVs and nodes for triangular grids with Donald polygons

For three-dimensional problems on the basis of hexahedral or tetrahedral grids similar techniques as in the two-dimensional case can be applied (see, e.g., [26]).

After having defined the CVs, the balance equations describing the problem are formulated in integral form for each CV. Normally, these equations are directly available from the corresponding continuum mechanical conservation laws (applied to a CV), but they can also be derived by integration from the corresponding differential equations. By integration of (4.1) over an arbitrary control volume  $V$  and application of the Gauß integral theorem, one obtains:

$$\int_S \left( \rho v_i \phi - \alpha \frac{\partial \phi}{\partial x_i} \right) n_i dS = \int_V f dV, \quad (4.2)$$

where  $S$  is the surface of the CV and  $n_i$  are the components of the unit normal vector to the surface. The integral balance equation (4.2) constitutes the starting point for the further discretization of the considered problem with an FVM.

As an example we consider quadrilateral CVs with a cell-oriented arrangement of nodes (a generalization to arbitrary polygons poses no principal difficulties). For a general quadrilateral CV we use the notations of the distinguished points (midpoint, midpoints of faces, and edge points) and the unit normal vectors according to the so-called compass notation as indicated in Fig. 4.5. The midpoints of the directly neighboring CVs we denote – again in compass notation – with capital letters S, SE, etc. (see Fig. 4.6).

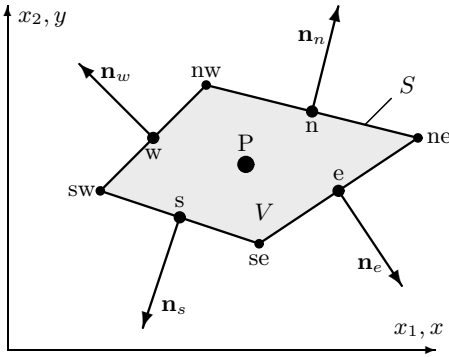


**Fig. 4.5.** Quadrilateral control volume with notations

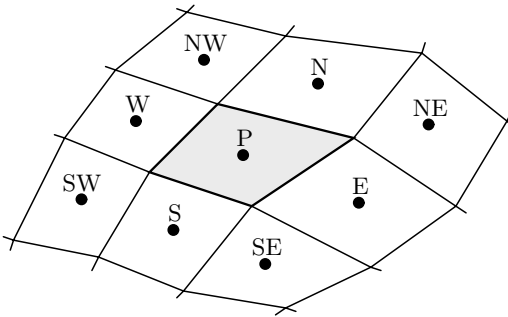


**Fig. 4.6.** Notations for neighboring control volumes

The surface integral in (4.2) can be split into the sum of the four surface integrals over the cell faces  $S_c$  ( $c = e, w, n, s$ ) of the CV, such that the balance equation (4.2) can be written equivalently in the form

$$\sum_c \int_{S_c} \left( \rho v_i \phi - \alpha \frac{\partial \phi}{\partial x_i} \right) n_{ci} dS_c = \int_V f dV. \tag{4.3}$$

The expression (4.3) represents a balance equation for the convective and diffusive fluxes  $F_c^C$  and  $F_c^D$  through the CV faces, respectively, with

$$F_c^C = \int_{S_c} (\rho v_i \phi) n_{ci} dS_c \quad \text{and} \quad F_c^D = - \int_{S_c} \left( \alpha \frac{\partial \phi}{\partial x_i} \right) n_{ci} dS_c .$$

For the face  $S_e$ , for instance, the unit normal vector  $\mathbf{n}_e = (n_{e1}, n_{e2})$  is defined by the following (geometric) conditions:

$$(\mathbf{x}_{ne} - \mathbf{x}_{se}) \cdot \mathbf{n}_e = 0 \quad \text{und} \quad |\mathbf{n}_e| = \sqrt{n_{e1}^2 + n_{e2}^2} = 1 .$$

From this one obtains the representation

$$\mathbf{n}_e = \frac{(y_{ne} - y_{se})}{\delta S_e} \mathbf{e}_1 - \frac{(x_{ne} - x_{se})}{\delta S_e} \mathbf{e}_2 , \tag{4.4}$$

where

$$\delta S_e = |\mathbf{x}_{ne} - \mathbf{x}_{se}| = \sqrt{(x_{ne} - x_{se})^2 + (y_{ne} - y_{se})^2}$$

denotes the length of the face  $S_e$ . Analogous relations result for the other CV faces.

For neighboring CVs with a common face the absolute value of the total flux  $F_c = F_c^C + F_c^D$  through this face is identical, but the sign differs. For instance, for the CV around point P the flux  $F_e$  is equal to the flux  $-F_w$  for the CV around point E (since  $(\mathbf{n}_e)_P = -(\mathbf{n}_w)_E$ ). This is exploited for the implementation of the method in order to avoid on the one hand a double computation for the fluxes and on the other hand to ensure that the corresponding absolute fluxes really are equal (important for conservativity, see Sect. 8.1.4). In the case of quadrilateral CVs the computation can be organized in such a way that, starting from a CV face at the boundary of the problem domain, for instance, only  $F_e$  and  $F_n$  have to be computed.

It should be noted that up to this point we haven't introduced any approximation, i.e., the flux balance (4.3) is still exact. The actual discretization now mainly consists in the approximation of the surface integrals and the volume integral in (4.3) by suitable averages of the corresponding integrands at the CV faces. Afterwards, these have to be put into proper relation to the unknown function values in the nodes.

## 4.2 Approximation of Surface and Volume Integrals

We start with the approximation of the surface integrals in (4.3), which for a cell-centered variable arrangement suitably is carried out in two steps:

- (1) Approximation of the surface integrals (fluxes) by values on the CV faces.

(2) Approximation of the variable values at the CV faces by node values.

As an example let us consider the approximation of the surface integral

$$\int_{S_e} w_i n_{ei} \, dS_e$$

over the face  $S_e$  of a CV for a general integrand function  $\mathbf{w} = (w_1(\mathbf{x}), w_2(\mathbf{x}))$  (the other faces can be treated in a completely analogous way).

The integral can be approximated in different ways by involving more or less values of the integrand at the CV face. The simplest possibility is an approximation by just using the midpoint of the face:

$$\int_{S_e} w_i n_{ei} \, dS_e \approx g_e \delta S_e, \quad (4.5)$$

where we denote with  $g_e = w_{ei} n_{ei}$  the normal component of  $\mathbf{w}$  at the location  $e$ . With this, one obtains an approximation of 2nd order (with respect to the face length  $\delta S_e$ ) for the surface integral, which can be checked by means of a Taylor series expansion (Exercise 4.1). The integration formula (4.5) corresponds to the *midpoint rule* known from numerical integration.

Other common integration formulas, that can be employed for such approximations are, for instance, the *trapezoidal rule* and the *Simpson rule*. The corresponding formulas are summarized in Table 4.1 with their respective orders (with respect to  $\delta S_e$ ).

**Table 4.1.** Approximations for surface integrals over the face  $S_e$

Name	Formula	Order
Midpoint rule	$\delta S_e g_e$	2
Trapezoidal rule	$\delta S_e (g_{ne} + g_{se})/2$	2
Simpson rule	$\delta S_e (g_{ne} + 4g_e + g_{se})/6$	4

For instance, by applying the midpoint rule for the approximation of the convective and diffusive fluxes through the CV faces in (4.3), we obtain the approximations:

$$F_c^C \approx \underbrace{\rho v_i n_{ci} \delta S_c}_{\dot{m}_c} \phi_c \quad \text{and} \quad F_c^D \approx -\alpha n_{ci} \delta S_c \left( \frac{\partial \phi}{\partial x_i} \right)_c,$$

where, for simplicity, we have assumed that  $v_i$ ,  $\rho$ , and  $\alpha$  are constant across the CV.  $\dot{m}_c$  denotes the mass flux through the face  $S_c$ . Inserting the definition

of the normal vector, we obtain, for instance, for the convective flux through the face  $S_e$ , the approximation

$$F_e^C \approx \dot{m}_e \phi_e = \rho [v_1(y_{ne} - y_{se}) - v_2(x_{ne} - x_{se})].$$

Before we turn to the further discretization of the fluxes, we first deal with the approximation of the volume integral in (4.3), which normally also is carried out by means of numerical integration. The assumption that the value  $f_P$  of  $f$  in the CV center represents an average value over the CV leads to the two-dimensional midpoint rule:

$$\int_V f \, dV \approx f_P \, \delta V,$$

where  $\delta V$  denotes the volume of the CV, which for a quadrilateral CV is given by

$$\delta V = \frac{1}{2} |(x_{se} - x_{nw})(y_{ne} - y_{sw}) - (x_{ne} - x_{sw})(y_{se} - y_{nw})|.$$

An overview of the most common two-dimensional integration formulas for Cartesian CVs with the corresponding error order (with respect to  $\delta V$ ) is given in Fig. 4.7 showing a schematical representation with the corresponding location of integration points and weighting factors. As a formula this means, e.g., in the case of the Simpson rule, an approximation of the form:

$$\int_V f \, dV \approx \frac{\delta V}{36} (16f_P + 4f_e + 4f_w + 4f_n + 4f_s + f_{ne} + f_{se} + f_{nw} + f_{sw}).$$

It should be noted that the formulas for the two-dimensional numerical integration can be used to approximate the surface integrals occurring in three-dimensional applications. For three-dimensional volume integrals analogous integration formulas as for the two-dimensional case are available.

In summary, by applying the midpoint rule (to which we will restrict ourselves) we now have the following approximation for the balance equation (4.3):

$$\underbrace{\sum_c \dot{m}_c \phi_c}_{\text{conv. fluxes}} - \underbrace{\sum_c \alpha n_{ci} \delta S_c \left( \frac{\partial \phi}{\partial x_i} \right)_c}_{\text{diff. fluxes}} = \underbrace{f_P \delta V}_{\text{source}} \quad (4.6)$$

In the next step it is necessary to approximate the function values and derivatives of  $\phi$  at the CV faces occurring in the convective and diffusive flux expressions, respectively, by variable values in the nodes (here the CV centers). In order to clearly outline the essential principles, we will first explain the corresponding approaches for a two-dimensional Cartesian CV as indicated in Fig. 4.8. In this case the unit normal vectors  $\mathbf{n}_c$  along the CV faces are given by

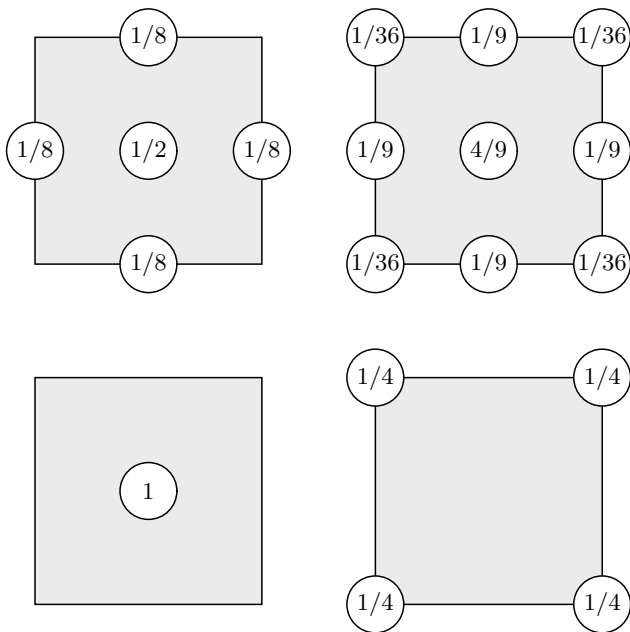


**Fig. 4.7.** Schematic representation of numerical integration formulas for two-dimensional volume integrals over a Cartesian CV

$$\mathbf{n}_e = \mathbf{e}_1, \quad \mathbf{n}_w = -\mathbf{e}_1, \quad \mathbf{n}_n = \mathbf{e}_2, \quad \mathbf{n}_s = -\mathbf{e}_2$$

and the expressions for the mass fluxes through the CV faces simplify to

$$\begin{aligned} \dot{m}_e &= \rho v_1(y_n - y_s), & \dot{m}_n &= \rho v_2(x_e - x_w), \\ \dot{m}_w &= \rho v_1(y_s - y_n), & \dot{m}_s &= \rho v_2(x_w - x_e). \end{aligned}$$

Particularities that arise due to non-Cartesian grids will be considered in Sect. 4.5.

### 4.3 Discretization of Convective Fluxes

For the further approximation of the convective fluxes  $F_c^C$ , it is necessary to approximate  $\phi_c$  by variable values in the CV centers. In general, this involves using neighboring nodal values  $\phi_E, \phi_P, \dots$  of  $\phi_c$ . The methods most frequently employed in practice for the approximation will be explained in the following, where we can restrict ourselves to one-dimensional considerations for the face  $S_e$ , since the other faces and the second (or third) spatial dimension can be treated in a fully analogous way. Traditionally, the corresponding approximations are called differencing techniques, since they result

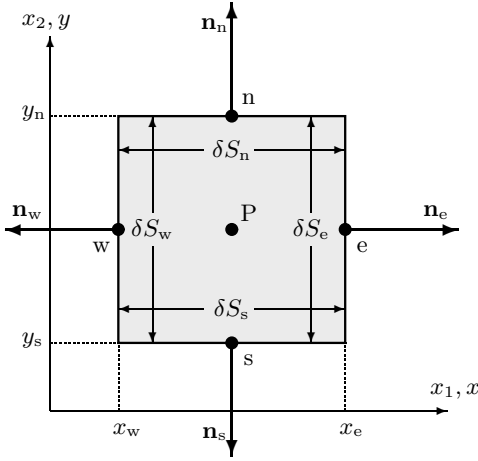


**Fig. 4.8.** Cartesian control volume with notations

in formulas analogous to finite-difference methods. Strictly speaking, these are interpolation techniques.

### 4.3.1 Central Differences

For the *central differencing scheme (CDS)*  $\phi_e$  is approximated by linear interpolation with the values in the neighboring nodes P and E (see Fig. 4.9):

$$\phi_e \approx \gamma_e \phi_E + (1 - \gamma_e) \phi_P. \tag{4.7}$$

The interpolation factor  $\gamma_e$  is defined by

$$\gamma_e = \frac{x_e - x_P}{x_E - x_P}.$$

The approximation (4.7) has, for an equidistant grid as well as for a non-equidistant grid, an interpolation error of 2nd order. This can be seen from a Taylor series expansion of  $\phi$  around the point  $x_P$ :

$$\phi(x) = \phi_P + (x - x_P) \left( \frac{\partial \phi}{\partial x} \right)_P + \frac{(x - x_P)^2}{2} \left( \frac{\partial^2 \phi}{\partial x^2} \right)_P + T_H,$$

where  $T_H$  denotes the terms of higher order. Evaluating this series at the locations  $x_e$  and  $x_E$  and taking the difference leads to the relation

$$\phi_e = \gamma_e \phi_E + (1 - \gamma_e) \phi_P - \frac{(x_e - x_P)(x_E - x_e)}{2} \left( \frac{\partial^2 \phi}{\partial x^2} \right)_P + T_H,$$

which shows that the leading error term depends quadratically on the grid spacing.

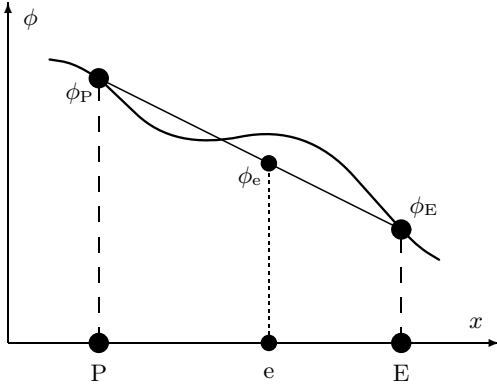


**Fig. 4.9.** Approximation of  $\phi_e$  with CDS method

By involving additional grid points, central differencing schemes of higher order can be defined. For instance, an approximation of 4th order for an equidistant grid is given by

$$\phi_e = \frac{1}{48}(-3\phi_{EE} + 27\phi_E + 27\phi_P - 3\phi_W),$$

where EE denotes the “east” neighboring point of E (see Fig. 4.11). Note that an application of this formula only makes sense if it is used together with an integration formula of 4th order, e.g., the Simpson rule. Only in this case is the total approximation of the convective flux also of 4th order.

When using central differencing approximations unphysical oscillations may appear in the numerical solution (the reasons for this problem will be discussed in detail in Sect. 8.1). Therefore, one often uses so-called *upwind approximations*, which are not sensitive or less sensitive to this problem. The principal idea of these methods is to make the interpolation dependent on the direction of the velocity vector. Doing so, one exploits the transport property of convection processes, which means that the convective transport of  $\phi$  only takes place “downstream”. In the following we will discuss two of the most important upwind techniques.

### 4.3.2 Upwind Techniques

The simplest upwind method results if  $\phi$  is approximated by a step function. Here,  $\phi_e$  is determined depending on the direction of the mass flux as follows (see Fig. 4.10):

$$\begin{aligned} \phi_e &= \phi_P, & \text{if } \dot{m}_e > 0, \\ \phi_e &= \phi_E, & \text{if } \dot{m}_e < 0. \end{aligned}$$

This method is called *upwind differencing scheme (UDS)*. A Taylor series expansion of  $\phi$  around the point  $x_P$ , evaluated at the point  $x_e$ , gives:

$$\phi_e = \phi_P + (x_e - x_P) \left( \frac{\partial \phi}{\partial x} \right)_P + \frac{(x_e - x_P)^2}{2} \left( \frac{\partial^2 \phi}{\partial x^2} \right)_P + T_H.$$

This shows that the UDS method (independent of the grid) has an interpolation error of 1st order. The leading error term in the resulting approximation of the convective flux  $F_e^C$  becomes

$$\underbrace{\dot{m}_e(x_e - x_P)}_{\alpha_{\text{num}}} \left( \frac{\partial \phi}{\partial x} \right)_P.$$

The error caused by this is called *artificial* or *numerical diffusion*, since the error term can be interpreted as a diffusive flux. The coefficient  $\alpha_{\text{num}}$  is a measure for the amount of the numerical diffusion. If the transport direction is nearly perpendicular to the CV face, the approximation of the convective fluxes resulting with the UDS method is comparably good (the derivative  $(\partial\phi/\partial x)_P$  is then small). Otherwise the approximation can be quite inaccurate and for large mass fluxes (i.e., large velocities) it can then be necessary to employ very fine grids (i.e.,  $x_e - x_P$  very small) for the computation in order to achieve a solution with an adequate accuracy. The disadvantage of the relatively poor accuracy is confronted by the advantage that the UDS method leads to an unconditionally bounded solution algorithm. We will discuss this aspect in more detail in Sect. 8.1.5.

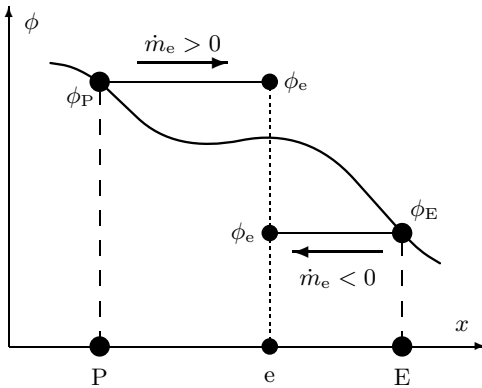


**Fig. 4.10.** Mass flux dependent approximation of  $\phi_e$  with UDS method

An upwind approximation frequently employed in practice is the quadratic upwind interpolation, which in the literature is known as the QUICK method (Quadratic Upwind Interpolation for Convective Kinematics). Here, a quadratic polynomial is fitted through the two neighboring points P and E, and a third point, which is located upwind (W or EE depending on the flow direction). Evaluating this polynomial at point e one obtains the approximation (see also Fig. 4.11):

$$\begin{aligned} \phi_e &= a_1\phi_E - a_2\phi_W + (1 - a_1 + a_2)\phi_P, & \text{if } \dot{m}_e > 0, \\ \phi_e &= b_1\phi_P - b_2\phi_{EE} + (1 - b_1 + b_2)\phi_E, & \text{if } \dot{m}_e < 0, \end{aligned}$$

where

$$\begin{aligned} a_1 &= \frac{(2 - \gamma_w)\gamma_e^2}{1 + \gamma_e - \gamma_w}, & a_2 &= \frac{(1 - \gamma_e)(1 - \gamma_w)^2}{1 + \gamma_e - \gamma_w}, \\ b_1 &= \frac{(1 + \gamma_w)(1 - \gamma_e)^2}{1 + \gamma_{ee} - \gamma_e}, & b_2 &= \frac{\gamma_{ee}^2\gamma_e}{1 + \gamma_{ee} - \gamma_e}. \end{aligned}$$

For an equidistant grid one has:

$$a_1 = \frac{3}{8}, \quad a_2 = \frac{1}{8}, \quad b_1 = \frac{3}{8}, \quad b_2 = \frac{1}{8}.$$

In this case the QUICK method possesses an interpolation error of 3rd order. However, if it is used together with numerical integration of only 2nd order the overall flux approximation also is only of 2nd order, but it is somewhat more accurate than with the CDS method.

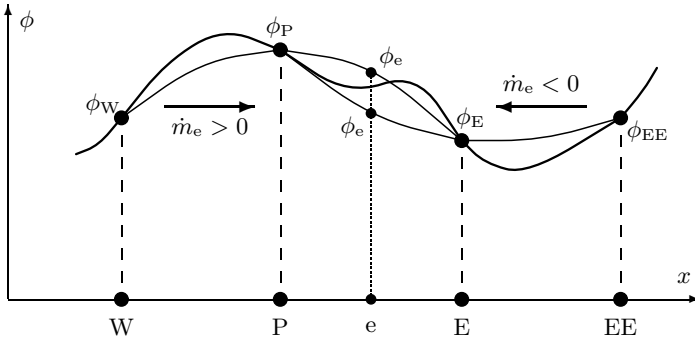


Fig. 4.11. Mass flux dependent approximation of  $\phi_e$  with QUICK method

Before we turn to the discretization of the diffusive fluxes, we will point to a special technique for the treatment of convective fluxes, which is frequently employed for transport equations.

### 4.3.3 Flux-Blending Technique

The principal idea of *flux-blending*, which goes back to Khosla und Rubin (1974), is to mix different approximations for the convective flux. In this way one attempts to combine the advantages of an accurate approximation of a higher order scheme with the better robustness and boundedness properties of a lower order scheme (mostly the UDS method).

To explain the method we again consider exemplarily the face  $S_e$  of a CV. The corresponding approximations for  $\phi_e$  in the convective flux  $F_e^C$  for the

two methods to be combined are denoted by  $\phi_e^{\text{ML}}$  and  $\phi_e^{\text{MH}}$ , where ML and MH are the lower and higher order methods, respectively. The approximation for the combined method reads:

$$\phi_e \approx (1 - \beta)\phi_e^{\text{ML}} + \beta\phi_e^{\text{MH}} = \phi_e^{\text{ML}} + \underbrace{\beta(\phi_e^{\text{MH}} - \phi_e^{\text{ML}})}_{b_\beta^{\phi,e}}. \quad (4.8)$$

From (4.8) for  $\beta=0$  and  $\beta=1$  the methods ML and MH, respectively, result. However, it is possible to choose for  $\beta$  any other value between 0 and 1, allowing to control the portions of the corresponding methods according to the needs of the underlying problem. However, due to the loss in accuracy, values  $\beta < 1$  should be selected only if with  $\beta = 1$  on the given grid no “reasonable” solution can be obtained (see Sect. 8.1.5) and a finer grid is not possible due to limitations in memory or computing time.

Also, if  $\beta = 1$  (i.e., the higher order method) is employed, it can be beneficial to use the splitting according to (4.8) in order to treat the term  $b_\beta^{\phi,e}$  “explicitly” in combination with an iterative solver. This means that this term is computed with (known) values of  $\phi$  from the preceding iteration and added to the source term. This may lead to a more stable iterative solution procedure, since this (probably critical) term then makes no contribution to the system matrix, which becomes more diagonally dominant. It should be pointed out that this modification has no influence on the converged solution, which is identical to that obtained with the higher order method MH alone. We will discuss this approach in some more detail at the end of Sect. 7.1.4.

## 4.4 Discretization of Diffusive Fluxes

For the approximation of diffusive fluxes it is necessary to approximate the values of the normal derivative of  $\phi$  at the CV faces by nodal values in the CV centers. For the east face  $S_e$  of the CV, which we will again consider exemplarily, one has to approximate (in the Cartesian case) the derivative  $(\partial\phi/\partial x)_e$ . For this, difference formulas as they are common in the framework of the finite-difference method can be used (see, e.g., [9]).

The simplest approximation one obtains when using a central differencing formula

$$\left(\frac{\partial\phi}{\partial x}\right)_e \approx \frac{\phi_E - \phi_P}{x_E - x_P}, \quad (4.9)$$

which is equivalent to the assumption that  $\phi$  is a linear function between the points  $x_P$  and  $x_E$  (see Fig. 4.12). For the discussion of the error of this approximation, we consider the difference of the Taylor series expansion around  $x_e$  at the locations  $x_P$  and  $x_E$ :

$$\left(\frac{\partial\phi}{\partial x}\right)_e = \frac{\phi_E - \phi_P}{x_E - x_P} + \frac{(x_e - x_P)^2 - (x_E - x_e)^2}{2(x_E - x_P)} \left(\frac{\partial^2\phi}{\partial x^2}\right)_e - \frac{(x_e - x_P)^3 + (x_E - x_e)^3}{6(x_E - x_P)} \left(\frac{\partial^3\phi}{\partial x^3}\right)_e + T_H.$$

One can observe that for an equidistant grid an error of 2nd order results, since in this case the coefficient in front of the second derivative is zero. In the case of non-equidistant grids, one obtains by a simple algebraic rearrangement that this leading error term is proportional to the grid spacing and the expansion rate  $\xi_e$  of neighboring grid spacings:

$$\frac{(1 - \xi_e)(x_e - x_P)}{2} \left(\frac{\partial^2\phi}{\partial x^2}\right)_e \quad \text{with} \quad \xi_e = \frac{x_E - x_e}{x_e - x_P}.$$

This means that the portion of the 1st order error term gets larger the more the expansion rate deviates from 1. This aspect should be taken into account in the grid generation such that neighboring CVs do not differ that much in the corresponding dimensions (see also Sect. 8.3).

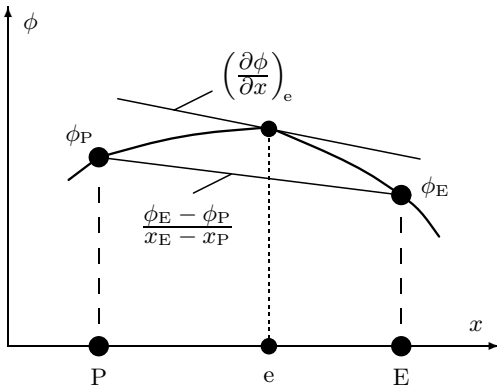


**Fig. 4.12.** Central differencing formula for approximation of 1st derivative at CV face

One obtains a 4th order approximation of the derivative at the CV face for an equidistant grid by

$$\left(\frac{\partial\phi}{\partial x}\right)_e \approx \frac{1}{24\Delta x} (\phi_W - 27\phi_P + 27\phi_E - \phi_{EE}), \tag{4.10}$$

which, for instance, can be used together with the Simpson rule to obtain an overall approximation for the diffusive flux of 4th order.

Although principally there are also other possibilities for approximating the derivatives (e.g., forward or backward differencing formulas), in practice almost only central differencing formulas are employed, which possess the best accuracy for a given number of grid points involved in the discretization. Problems with boundedness, as for the convective fluxes, do not exist. Thus,

there is no reason to use less accurate approximations. For CVs located at the boundary of the problem domain, it might be necessary to employ forward or backward differencing formulas because there are no grid points beyond the boundary (see Sect. 4.7).

## 4.5 Non-Cartesian Grids

The previous considerations with respect to the discretization of the convective and diffusive fluxes were confined to the case of Cartesian grids. In this section we will discuss necessary modifications for general (quadrilateral) CVs.

For the convective fluxes, simple generalizations of the schemes introduced in Sect. 4.3 (e.g., UDS, CDS, QUICK, ...) can be employed for the approximation of  $\phi_c$ . For instance, a corresponding CDS approximation for  $\phi_e$  reads:

$$\phi_e \approx \frac{|\mathbf{x}_{\tilde{e}} - \mathbf{x}_P|}{|\mathbf{x}_E - \mathbf{x}_P|} \phi_E + \frac{|\mathbf{x}_E - \mathbf{x}_{\tilde{e}}|}{|\mathbf{x}_E - \mathbf{x}_P|} \phi_P, \quad (4.11)$$

where  $\mathbf{x}_{\tilde{e}}$  is the intersection of the connecting line of the points P and E with the (probably extended) CV face  $S_e$  (see Fig. 4.13). For the convective flux through  $S_e$  this results in the following approximation:

$$F_e^C \approx \frac{\dot{m}_e}{|\mathbf{x}_E - \mathbf{x}_P|} (|\mathbf{x}_{\tilde{e}} - \mathbf{x}_P| \phi_E + |\mathbf{x}_E - \mathbf{x}_{\tilde{e}}| \phi_P).$$

When the grid at the corresponding face has a “kink”, an additional error results because the points  $\mathbf{x}_{\tilde{e}}$  and  $\mathbf{x}_e$  do not coincide (see Fig. 4.13). This aspect should be taken into account for the grid generation (see also Sect. 8.3).

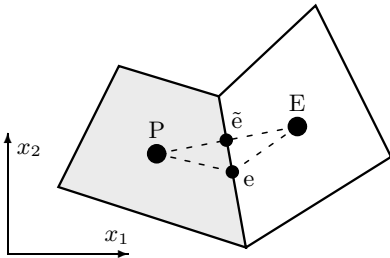


**Fig. 4.13.** Central difference approximation of convective fluxes for non-Cartesian control volumes

Let us turn to the approximation of the diffusive fluxes, for which farther reaching distinctions to the Cartesian case arise as for the convective fluxes. Here, for the required approximation of the normal derivative of  $\phi$  in the center of the CV face there are a variety of different possibilities, depending on the directions in which the derivative is approximated, the locations where the appearing derivatives are evaluated, and the node values which are used

for the interpolation. As an example we will give here one variant and consider only the CV face  $S_e$ .

Since along the normal direction in general there are no nodal points, the normal derivative has to be expressed by derivatives along other suitable directions. For this we use here the coordinates  $\tilde{\xi}$  and  $\tilde{\eta}$  defined according to Fig. 4.14. The direction  $\tilde{\xi}$  is determined by the connecting line between points P and E, and the direction  $\tilde{\eta}$  is determined by the direction of the CV face. Note that  $\tilde{\xi}$  and  $\tilde{\eta}$ , because of a distortion of the grid, can deviate from the directions  $\xi$  and  $\eta$ , which are defined by the connecting lines of P with the CV face centers e and n. The larger these deviations are, the larger the discretization error becomes. This is another aspect that has to be taken into account when generating the grid (see also Sect. 8.3).

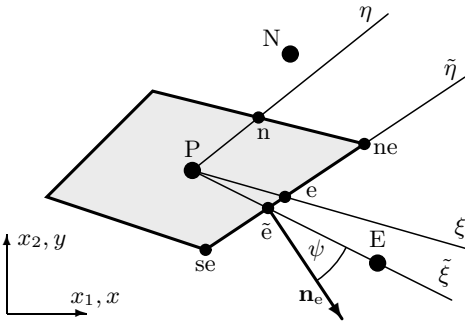


**Fig. 4.14.** Approximation of diffusive fluxes for non-Cartesian control volumes

A coordinate transformation  $(x, y) \rightarrow (\tilde{\xi}, \tilde{\eta})$  results for the normal derivative in the following representation:

$$\frac{\partial \phi}{\partial x} n_{e1} + \frac{\partial \phi}{\partial y} n_{e2} = \frac{1}{J} \left[ \left( \frac{\partial y}{\partial \tilde{\eta}} n_{e1} - \frac{\partial x}{\partial \tilde{\eta}} n_{e2} \right) \frac{\partial \phi}{\partial \tilde{\xi}} + \left( \frac{\partial x}{\partial \tilde{\xi}} n_{e2} - \frac{\partial y}{\partial \tilde{\xi}} n_{e1} \right) \frac{\partial \phi}{\partial \tilde{\eta}} \right] \quad (4.12)$$

with the Jacobi determinant

$$J = \frac{\partial x}{\partial \tilde{\xi}} \frac{\partial y}{\partial \tilde{\eta}} - \frac{\partial y}{\partial \tilde{\xi}} \frac{\partial x}{\partial \tilde{\eta}}.$$

The metric quantities can be approximated according to

$$\frac{\partial \mathbf{x}}{\partial \tilde{\xi}} \approx \frac{\mathbf{x}_E - \mathbf{x}_P}{|\mathbf{x}_E - \mathbf{x}_P|} \quad \text{and} \quad \frac{\partial \mathbf{x}}{\partial \tilde{\eta}} \approx \frac{\mathbf{x}_{ne} - \mathbf{x}_{se}}{\delta S_e}, \quad (4.13)$$

which results for the Jacobi determinant in the approximation

$$J_e \approx \frac{(x_E - x_P)(y_{ne} - y_{se}) - (y_E - y_P)(x_{ne} - x_{se})}{|\mathbf{x}_E - \mathbf{x}_P| \delta S_e} = \cos \psi,$$

where  $\psi$  denotes the angle between the direction  $\tilde{\xi}$  and  $\mathbf{n}_e$  (see Fig. 4.14).  $\psi$  is a measure for the deviation of the grid from orthogonality ( $\psi = 0$  for an orthogonal grid).

The derivatives with respect to  $\tilde{\xi}$  and  $\tilde{\eta}$  in (4.12) can be approximated in the usual way with a finite-difference formula. For example, the use of a central difference of 2nd order gives:

$$\frac{\partial\phi}{\partial\tilde{\xi}} \approx \frac{\phi_E - \phi_P}{|\mathbf{x}_E - \mathbf{x}_P|} \quad \text{and} \quad \frac{\partial\phi}{\partial\tilde{\eta}} \approx \frac{\phi_{ne} - \phi_{se}}{\delta S_e}. \quad (4.14)$$

Inserting the approximations (4.13) and (4.14) into (4.12) and using the component representation (4.4) of the unit normal vector  $\mathbf{n}_e$  we finally obtain the following approximation for the diffusive flux through the CV face  $S_e$ :

$$F_e^D \approx D_e(\phi_E - \phi_P) + N_e(\phi_{ne} - \phi_{se}) \quad (4.15)$$

with

$$D_e = \frac{\alpha [(y_{ne} - y_{se})^2 + (x_{ne} - x_{se})^2]}{(x_{ne} - x_{se})(y_E - y_P) - (y_{ne} - y_{se})(x_E - x_P)}, \quad (4.16)$$

$$N_e = \frac{\alpha [(y_{ne} - y_{se})(y_E - y_P) + (x_{ne} - x_{se})(x_E - x_P)]}{(y_{ne} - y_{se})(x_E - x_P) - (x_{ne} - x_{se})(y_E - y_P)}. \quad (4.17)$$

The coefficient  $N_e$  represents the portion that arise due to the non-orthogonality of the grid. If the grid is orthogonal,  $\mathbf{n}_e$  and  $\mathbf{x}_E - \mathbf{x}_P$  have the same direction such that  $N_e = 0$ . The coefficient  $N_e$  (and the corresponding values for the other CV faces) should be kept as small as possible (see als Sect. 8.3).

The values for  $\phi_{ne}$  and  $\phi_{se}$  in (4.15) can be approximated, for instance, by linear interpolation of four neighboring nodal values:

$$\phi_{ne} = \frac{\gamma_P\phi_P + \gamma_E\phi_E + \gamma_N\phi_N + \gamma_{NE}\phi_{NE}}{\gamma_P + \gamma_E + \gamma_N + \gamma_{NE}}$$

with suitable interpolation factors  $\gamma_P, \gamma_E, \gamma_N,$  and  $\gamma_{NE}$  (see Fig. 4.15).

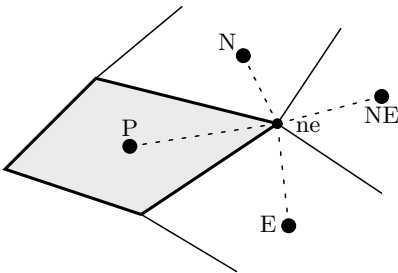


**Fig. 4.15.** Interpolation of values in CV edges for discretization of diffusive fluxes for non-Cartesian CV

## 4.6 Discrete Transport Equation

Let us now return to our example of the general two-dimensional transport equation (4.3) and apply the approximation techniques introduced in the preceding sections to it.

We employ exemplarily the midpoint rule for the integral approximations, the UDS method for the convective flux, and the CDS method for the diffusive flux. Additionally, we assume that we have velocity components  $v_1, v_2 > 0$  and that the grid is a Cartesian one. With these assumptions one obtains the following approximation of the balance equation (4.3):

$$\begin{aligned} & \left( \rho v_1 \phi_P - \alpha \frac{\phi_E - \phi_P}{x_E - x_P} \right) (y_n - y_s) \\ & - \left( \rho v_1 \phi_W - \alpha \frac{\phi_P - \phi_W}{x_P - x_W} \right) (y_n - y_s) \\ & + \left( \rho v_2 \phi_P - \alpha \frac{\phi_N - \phi_P}{y_N - y_P} \right) (x_e - x_w) \\ & - \left( \rho v_2 \phi_S - \alpha \frac{\phi_P - \phi_S}{y_P - y_S} \right) (x_e - x_w) = f_P (y_n - y_s) (x_e - x_w). \end{aligned}$$

A simple rearrangement gives a relation of the form

$$a_P \phi_P = a_E \phi_E + a_W \phi_W + a_N \phi_N + a_S \phi_S + b_P \quad (4.18)$$

with the coefficients

$$\begin{aligned} a_E &= \frac{\alpha}{(x_E - x_P)(x_e - x_w)}, \\ a_W &= \frac{\rho v_1}{x_e - x_w} + \frac{\alpha}{(x_P - x_W)(x_e - x_w)}, \\ a_N &= \frac{\alpha}{(y_N - y_P)(y_n - y_s)}, \\ a_S &= \frac{\rho v_2}{y_n - y_s} + \frac{\alpha}{(y_P - y_S)(y_n - y_s)}, \\ a_P &= \frac{\rho v_1}{x_e - x_w} + \frac{\alpha(x_E - x_W)}{(x_P - x_W)(x_E - x_P)(x_e - x_w)} + \\ & \quad \frac{\rho v_2}{y_n - y_s} + \frac{\alpha(y_N - y_S)}{(y_P - y_S)(y_N - y_P)(y_n - y_s)}, \\ b_P &= f_P. \end{aligned}$$

If the grid is equidistant in each spatial direction (with grid spacings  $\Delta x$  and  $\Delta y$ ), the coefficients become:

$$\begin{aligned} a_E &= \frac{\alpha}{\Delta x^2}, \quad a_W = \frac{\rho v_1}{\Delta x} + \frac{\alpha}{\Delta x^2}, \quad a_N = \frac{\alpha}{\Delta y^2}, \quad a_S = \frac{\rho v_2}{\Delta y} + \frac{\alpha}{\Delta y^2}, \\ a_P &= \frac{\rho v_1}{\Delta x} + \frac{2\alpha}{\Delta x^2} + \frac{\rho v_2}{\Delta y} + \frac{2\alpha}{\Delta y^2}, \quad b_P = f_P. \end{aligned}$$

In this particular case (4.18) coincides with a discretization that would result from a corresponding finite-difference method (for general grids this normally is not the case).

It can be seen that – independent from the grid employed – one has for the coefficients in (4.18) the relation

$$a_P = a_E + a_W + a_N + a_S .$$

This is characteristic for finite-volume discretizations and expresses the conservativity of the method. We will return to this important property in Sect. 8.1.4.

Equation (4.18) is valid in this form for all CVs, which are not located at the boundary of the problem domain. For boundary CVs the approximation (4.18) includes nodal values outside the problem domain, such that they require a special treatment depending on the given type of boundary condition.

## 4.7 Treatment of Boundary Conditions

We consider the three boundary condition types that most frequently occur for the considered type of problems (see Chap. 2): a prescribed variable value, a prescribed flux, and a symmetry boundary. For an explanation of the implementation of such conditions into a finite-volume method, we consider as an example a Cartesian CV at the west boundary (see Fig. 4.16) for the transport equation (4.3). Correspondingly modified approaches for the non-Cartesian case or for other types of equations can be formulated analogously (for this see also Sect. 10.4).

Let us start with the case of a prescribed boundary value  $\phi_w = \phi^0$ . For the convective flux at the boundary one has the approximation:

$$F_w^C \approx \dot{m}_w \phi_w = \dot{m}_w \phi^0 .$$

With this the approximation of  $F_w^C$  is known (the mass flux  $\dot{m}_w$  at the boundary is also known) and can simply be introduced in the balance equation (4.6). This results in an additional contribution to the source term  $b_P$ .

The diffusive flux through the boundary is determined with the same approach as in the interior of the domain (see (4.18)). Analogously to (4.9) the derivative at the boundary can be approximated as follows:

$$\left( \frac{\partial \phi}{\partial x} \right)_w \approx \frac{\phi_P - \phi_w}{x_P - x_w} = \frac{\phi_P - \phi^0}{x_P - x_w} . \quad (4.19)$$

This corresponds to a forward difference formula of 1st order. Of course, it is also possible to apply more elaborate formulas of higher order. However, since the distance between the boundary point  $w$  and the point  $P$  is smaller than

the distance between two inner points (half as much for an equidistant grid, see Fig. 4.16), a lower order approximation at the boundary usually does not influence the overall accuracy that much.

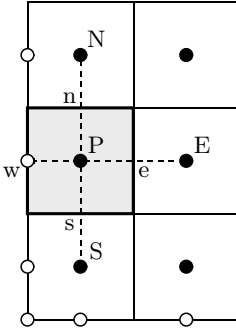


**Fig. 4.16.** Cartesian boundary CV at west boundary with notations

In summary, one has for the considered boundary CV a relation of the form (4.18) with the modified coefficients:

$$\begin{aligned}
 a_W &= 0, \\
 a_P &= \frac{\rho v_1}{x_e - x_w} + \frac{\alpha(x_E - x_w)}{(x_P - x_w)(x_E - x_P)(x_e - x_w)} + \\
 &\quad \frac{\rho v_2}{y_n - y_s} + \frac{\alpha(y_N - y_S)}{(y_P - y_S)(y_N - y_P)(y_n - y_s)}, \\
 b_P &= f_P + \left[ \frac{\rho v_1}{x_e - x_w} + \frac{\alpha}{(x_P - x_w)(x_e - x_w)} \right] \phi^0.
 \end{aligned}$$

All other coefficients are computed as for a CV in the interior of the problem domain.

Let us now consider the case where the flux  $F_w = F^0$  is prescribed at the west boundary. The flux through the CV face is obtained by dividing  $F^0$  through the length of the face  $x_e - x_w$ . The resulting value is introduced in (4.6) as total flux and the modified coefficients for the boundary CV become:

$$\begin{aligned}
 a_W &= 0, \\
 a_P &= \frac{\rho v_1}{x_e - x_w} + \frac{\alpha}{(x_E - x_P)(x_e - x_w)} + \\
 &\quad \frac{\rho v_2}{y_n - y_s} + \frac{\alpha(y_N - y_S)}{(y_P - y_S)(y_N - y_P)(y_n - y_s)}, \\
 b_P &= f_P + \frac{F^0}{x_e - x_w}.
 \end{aligned}$$

All other coefficients remain unchanged.

Sometimes it is possible to exploit symmetries of a problem in order to downsize the problem domain to save computing time or get a higher accuracy

(with a finer grid) with the same computational effort. In such cases one has to consider symmetry planes or symmetry lines at the corresponding problem boundary. In this case one has the boundary condition:

$$\frac{\partial \phi}{\partial x_i} n_i = 0. \quad (4.20)$$

From this condition it follows that the diffusive flux through the symmetry boundary is zero (see (4.18)). Since also the normal component of the velocity vector has to be zero at a symmetry boundary (i.e.,  $v_i n_i = 0$ ), the mass flux and, therefore, the convective flux through the boundary is zero. Thus, in the balance equation (4.6) the total flux through the corresponding CV face can be set to zero. For the boundary CV in Fig. 4.16 this results in the following modified coefficients:

$$\begin{aligned} a_W &= 0, \\ a_P &= \frac{\rho v_1}{x_e - x_w} + \frac{\alpha}{(x_E - x_P)(x_e - x_w)} + \\ &\quad \frac{\rho v_2}{y_n - y_s} + \frac{\alpha(y_N - y_S)}{(y_P - y_S)(y_N - y_P)(y_n - y_s)}. \end{aligned}$$

If required, the (unknown) variable value at the boundary can be determined by a finite-difference approximation of the boundary condition (4.20). In the considered case, for instance, with a forward difference formula (cp. (4.19)) one simply obtains  $\phi_w = \phi_P$ .

As with all other discretization techniques, the algebraic system of equations resulting from a finite-volume discretization has a unique solution only if the boundary conditions at all boundaries of the problem domain are taken into account (e.g., as outlined above). Otherwise there would be more unknowns than equations.

## 4.8 Algebraic System of Equations

As exemplarily outlined in Sect. 4.6 for the general scalar transport equation, a finite-volume discretization for each CV results in an algebraic equation of the form:

$$a_P \phi_P - \sum_c a_c \phi_c = b_P,$$

where the index  $c$  runs over all neighboring points that are involved in the approximation as a result of the discretization scheme employed. Globally, i.e., for all control volumes  $V_i$  ( $i = 1, \dots, N$ ) of the problem domain, this gives a linear system of  $N$  equations







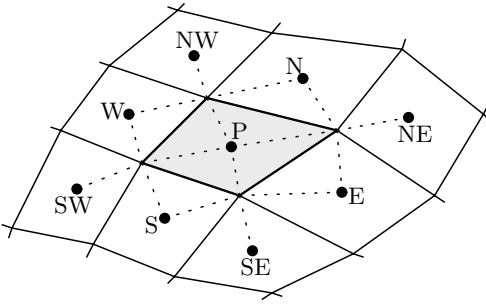


**Fig. 4.20.** Interpolation of vertex values for non-Cartesian CV

plate. At three sides the temperature  $T$  is prescribed and at the fourth side the heat flux is given (equal to zero). The problem data are summarized in Fig. 4.21. The problem is described by the heat conduction equation

$$-\kappa \frac{\partial^2 T}{\partial x^2} - \kappa \frac{\partial^2 T}{\partial y^2} = \rho q \tag{4.24}$$

with the boundary conditions as indicated in Fig. 4.21 (cp. Sect. 2.3.2). For the discretization we employ a grid with only two CVs as illustrated in Fig. 4.22. The required coordinates for the distinguished points for both CVs are indicated in Table 4.2.

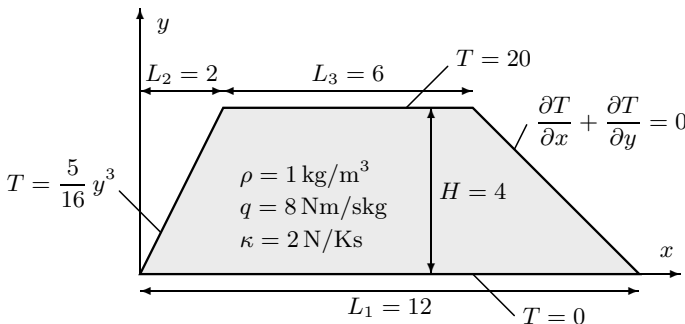


**Fig. 4.21.** Configuration of trapezoidal plate heat conduction example (temperature in K, length in m)

The integration of (4.24) over a control volume  $V$  and the application of the Gauß integral theorem gives:

$$\sum_c F_c = -\kappa \sum_c \int_{S_c} \left( \frac{\partial T}{\partial x} n_1 + \frac{\partial T}{\partial y} n_2 \right) dS_c = \int_V q dV,$$

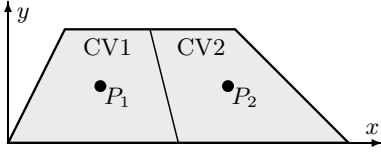


**Fig. 4.22.** CV definition for trapezoidal plate

**Table 4.2.** Coordinates of distinguished points for discretized trapezoidal plate

Point	CV1		CV2	
	$x$	$y$	$x$	$y$
P	13/4	2	31/4	2
e	11/2	2	10	2
w	1	2	11/2	2
n	7/2	4	13/2	4
s	3	0	9	0
nw	2	4	5	4
ne	5	4	8	4
se	6	0	12	0
sw	0	0	6	0
Volume	18		18	

where the summation has to be carried out over  $c = s, n, w, e$ . For the approximation of the integrals we employ the midpoint rule and the derivatives at CV faces are approximated by second-order central differences. Thus, the approximations of the fluxes for CV1 is:

$$\begin{aligned}
 F_e &= -\kappa \int_{S_e} \left( \frac{4}{\sqrt{17}} \frac{\partial T}{\partial x} + \frac{1}{\sqrt{17}} \frac{\partial T}{\partial y} \right) dS_e \approx \\
 &\approx D_e (T_E - T_P) + N_e (T_{ne} - T_{se}) = -\frac{17}{9} (T_E - T_P) - 10, \\
 F_w &= -\kappa \int_{S_w} \left( -\frac{2}{\sqrt{5}} \frac{\partial T}{\partial x} + \frac{1}{\sqrt{5}} \frac{\partial T}{\partial y} \right) dS_w = \\
 &= -\kappa \int_{S_w} \left( -\frac{2}{\sqrt{5}} \frac{120}{16} x^2 + \frac{1}{\sqrt{5}} \frac{15}{16} y^2 \right) dS_w = 60, \\
 F_s &= -\kappa \int_{S_s} \left( -\frac{\partial T}{\partial y} \right) dS_s \approx -\kappa \left( \frac{\partial T}{\partial y} \right)_s (x_{se} - x_{sw}) \approx \\
 &\approx -\kappa \left( \frac{T_P - T_S}{y_P - y_S} \right) (x_{se} - x_{sw}) = 6T_P,
 \end{aligned}$$

$$\begin{aligned}
 F_n &= -\kappa \int_{S_n} \frac{\partial T}{\partial y} dS_n \approx -\kappa \left( \frac{\partial T}{\partial y} \right)_n (x_{ne} - x_{nw}) \approx \\
 &\approx -\kappa \left( \frac{T_N - T_P}{y_N - y_P} \right) (x_{ne} - x_{nw}) = 3T_P - 60.
 \end{aligned}$$

The flux  $F_w$  has been computed exactly from the given boundary value function. Similarly, one obtains for CV2:

$$F_e = 0, \quad F_w \approx \frac{17}{9} (T_P - T_W) + 10, \quad F_s \approx 6T_P, \quad F_n \approx 3T_P - 60.$$

For both CVs we have  $\delta V = 18$ , such that the following discrete balance equations result:

$$\frac{98}{9} T_P - \frac{17}{9} T_E = 154 \quad \text{and} \quad \frac{98}{9} T_P - \frac{17}{9} T_W = 194.$$

We have  $T_P = T_1$  and  $T_E = T_2$  for CV1, and  $T_P = T_2$  and  $T_W = T_1$  for CV2. This gives the linear system of equations

$$98T_1 - 17T_2 = 1386 \quad \text{and} \quad 98T_2 - 17T_1 = 1746$$

for the two unknown temperatures  $T_1$  and  $T_2$ . Its solution gives  $T_1 \approx 17,77$  and  $T_2 \approx 20,90$ .

## Exercises for Chap. 4

**Exercise 4.1.** Determine the leading error terms for the one-dimensional midpoint and trapezoidal rules by Taylor series expansion and compare the results.

**Exercise 4.2.** Let the concentration of a pollutant  $\phi = \phi(x)$  in a chimney be described by the differential equation

$$-3\phi' - 2\phi'' = x \cos(\pi x) \quad \text{for} \quad 0 < x < 6$$

with the boundary conditions  $\phi'(0) = 1$  and  $\phi(6) = 2$ . Compute the values  $\phi_1$  and  $\phi_2$  in the centers of the two control volumes CV1 =  $[0, 4]$  and CV2 =  $[4, 6]$  with a finite-volume discretization using the UDS method for the convective term.

**Exercise 4.3.** Consider the heat conduction in a square plate with the problem data given in Fig. 4.23. Compute the solution with a finite-volume method for the two grids illustrated in Fig. 4.24. Compare the results with the analytic solution  $T_a(x, y) = 20 - 2y^2 + x^3y - xy^3$ .

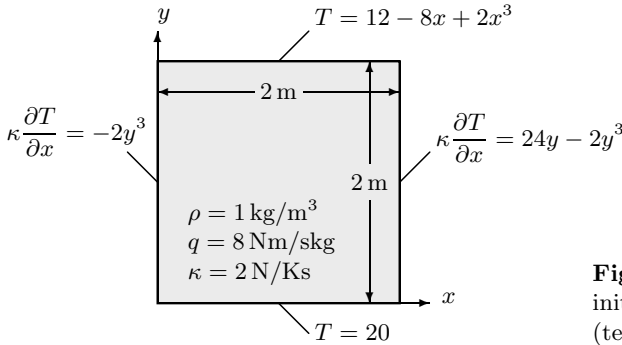


**Fig. 4.23.** Problem definition for Exercise 4.3 (temperatures in K)

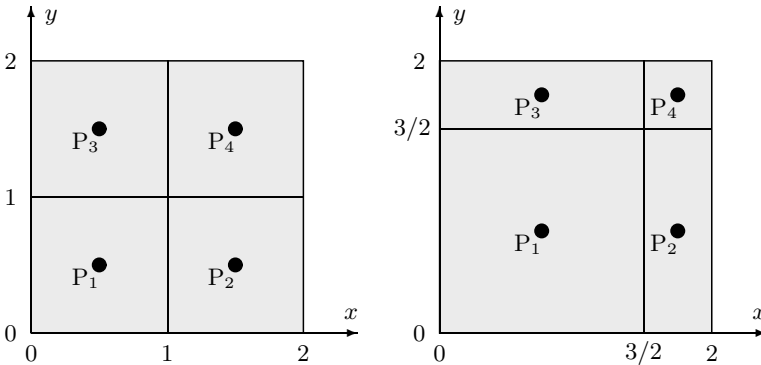


**Fig. 4.24.** Numerical grids for Exercise 4.3

**Exercise 4.4.** Formulate a finite-volume method of 2nd order for equidistant grids for the bar equation (2.38). Use this for computing the displacement of a bar of length  $L = 60 \text{ m}$  with the boundary conditions (2.39) with  $A(x) = 1 + x/60$ ,  $u_0 = 0$ , and  $k_L = 4 \text{ N}$  employing a discretization with three equidistant CVs.

**Exercise 4.5.** Formulate a finite-volume method of 4th order for the membrane equation (2.17) for an equidistant Cartesian grid.

**Exercise 4.6.** Consider the integral

$$I = \int_{S_e} \phi \, dS$$

for the function  $\phi = \phi(x, y)$  over the face  $S_e$  of the CV  $[1, 3]^2$ . (i) Determine the leading error term and the order (with respect to the length  $\Delta y$  of  $S_e$ ) for the approximation

$$I \approx \phi(3, \alpha) \Delta y$$

depending on the parameter  $\alpha \in [1, 3]$ . (ii) Compute  $I$  for the function  $\phi(x, y) = x^3y^4$  directly (analytically) and with the approximation defined in (i) with  $\alpha = 2$ . Compare the two solutions.

**Exercise 4.7.** The velocity vector of a two-dimensional flow is given by

$$\mathbf{v} = (v_1(x, y), v_2(x, y)) = (x \cos \pi y, x^4 y).$$

Let the flux through the surface  $S$  of the control volume  $V = [1, 2]^2$  be defined by

$$I = \int_S v_i n_i \, dS.$$

(i) Approximate the integral with the Simpson rule. (ii) Transform the integral with the Gauß integral theorem into a volume integral (over  $V$ ) and approximate this with the midpoint rule.



<http://www.springer.com/978-3-540-30685-6>

Computational Engineering - Introduction to Numerical  
Methods

Schäfer, M.

2006, X, 321 p. 204 illus., Softcover

ISBN: 978-3-540-30685-6